

Available online at [www.sciencedirect.com](http://www.sciencedirect.com)

ScienceDirect

journal homepage: [www.e-asianjournalsurgery.com](http://www.e-asianjournalsurgery.com)

## ORIGINAL ARTICLE

# Tumor suppressor miRNA-204-5p promotes apoptosis by targeting BCL2 in prostate cancer cells

Yi-Chia Lin <sup>a,b,e</sup>, Ji-Fan Lin <sup>c,e</sup>, Te-Fu Tsai <sup>a,b</sup>, Kuang-Yu Chou <sup>a,b</sup>,  
Hung-En Chen <sup>a</sup>, Thomas I-Sheng Hwang <sup>a,b,d,\*</sup>

<sup>a</sup> Department of Urology, Shin Kong Wu Ho-Su Memorial Hospital, Taipei, Taiwan

<sup>b</sup> School of Medicine, Fu-Jen Catholic University, New Taipei City, Taiwan

<sup>c</sup> Central Laboratory, Shin Kong Wu Ho-Su Memorial Hospital, Taipei, Taiwan

<sup>d</sup> School of Medicine, Taipei Medical University, Taipei, Taiwan

Received 20 November 2015; received in revised form 22 February 2016; accepted 23 March 2016

## KEYWORDS

apoptosis;  
BCL2;  
microRNAs;  
prostate cancer

**Summary** *Background:* Prostate cancer (PCa) is a leading cause of cancer-related death in men, which emphasizes the need for novel therapeutic approaches. Targeting microRNA (miRNA) has been considered as a therapeutic strategy against cancers. Human miR-204-5p potentially targeting BCL2 has been reported to be downregulated in various cancers. We hypothesized that miR-204-5p overexpression induces cancer cell apoptosis by repressing BCL2 expression.

*Methods:* A vector harboring mature miR-204-5p was constructed and delivered into human PCa cells. The expression level of miR-204-5p was determined by miRNA quantitative polymerase chain reaction (QPCR). Luciferase reporter assays were performed to verify the function of mature miR-204-5p and its direct binding to BCL2 transcripts. The expression levels of BCL2 messenger RNA (mRNA) and protein samples were measured by QPCR and Western blot, respectively. Cell viability was detected by WST-1 assays. Induction of apoptosis was determined by increased levels of cleavage caspase 3 and caspase 3/7 activity.

*Results:* The expression levels of miR-204-5p were downregulated in PCa cells compared with normal prostate epithelial cells. Transfection of pSM-204 resulted in up to 6.2-fold higher expression of miR-204-5p when compared with pSM control. The mRNA levels of several potential target genes of miR-204-5p were decreased in pSM-204-transfected PC3 and Rv1 cells. BCL2 mRNA and protein expression decreased in miR-204-5p-transfected cells, which led to cytochrome C release from mitochondria. It subsequently increased cleaved caspase 3 and caspase

Conflicts of interest: The authors declare no conflicts of interest.

\* Corresponding author. Division of Urology, Department of Surgery, Shin Kong Wu Ho-Su Memorial Hospital, No. 95, Wenchang Rd., Shilin Dist., Taipei City 111, Taiwan.

E-mail addresses: [M001009@ms.skh.org.tw](mailto:M001009@ms.skh.org.tw), [thomashwang0820@gmail.com](mailto:thomashwang0820@gmail.com) (T.I.-S. Hwang).

<sup>e</sup> Both authors contributed equally to this manuscript.

<http://dx.doi.org/10.1016/j.asjsur.2016.07.001>

1015-9584/Copyright © 2016, Asian Surgical Association. Published by Elsevier Taiwan LLC. This is an open access article under the CC BY-NC-ND license (<http://creativecommons.org/licenses/by-nc-nd/4.0/>).

Please cite this article in press as: Lin Y-C, et al., Tumor suppressor miRNA-204-5p promotes apoptosis by targeting BCL2 in prostate cancer cells, Asian Journal of Surgery (2016), <http://dx.doi.org/10.1016/j.asjsur.2016.07.001>

3/7 activities and reduced cell viability. Cotransfection of a reporter vector harboring the *BCL2* 3'-untranslated region to compete with endogenous transcripts partially rescued miR-204-5p-induced apoptosis.

**Conclusion:** Human miR-204-5p targets *BCL2* in PCa cells. Restoration of miR-204-5p in PCa could therefore be considered as a novel strategy by targeting antiapoptotic *BCL2*.

Copyright © 2016, Asian Surgical Association. Published by Elsevier Taiwan LLC. This is an open access article under the CC BY-NC-ND license (<http://creativecommons.org/licenses/by-nc-nd/4.0/>).

## 1. Introduction

The incidence and mortality of prostate cancer (PCa) in Asian populations have rapidly increased. It has become the sixth common cancer in Taiwan since 1996.<sup>1</sup> The age-adjusted incidence rate of PCa was reported to have increased 18-fold in 2012 compared with that in 1985.<sup>2</sup> Therefore, exploring the mechanisms of the initiation and progression of PCa may contribute to optimize the therapeutic strategies. Deregulation of epigenetic mechanism has been investigated as a relevant driving force in PCa over the past decades.<sup>3</sup> More recently, the expression of deregulated microRNAs (miRNAs) in PCa was revealed.<sup>4,5</sup>

miRNAs are approximately 22-nt long noncoding RNAs transcribed endogenously, which are involved in a new level of gene regulation. miRNAs play a role in gene regulation by cleaving or repressing the translation of their target messenger RNA (mRNAs) at the post-transcriptional level. Unlike transcriptional factors promoting gene expressions, miRNAs are recognized as negative regulators, which bind to their target mRNAs and suppress protein translation by either blocking translation or destabilizing mRNA.<sup>6</sup> miRNAs have been reported to be involved in many important biological functions. For example, miR-15a and miR-16 induce apoptosis by targeting *BCL2*; miR-375 is a pancreatic-specific miRNA that regulates insulin secretion.<sup>7,8</sup> Furthermore, high-throughput techniques such as microarray analysis revealed aberrant miRNA expression in numerous tumors compared with their normal counterparts, suggesting that there exists a link between miRNAs and cancer.<sup>9</sup>

In tumor cells, expression of miR-204-5p has been reported to be downregulated in several types of tumors.<sup>10,11</sup> The downregulation was suggested to contribute to tumor growth through the repression of miR-204-5p targets including *HOXA10* and *MEIS1*, as well as some predicted targets such as *BCL2*.<sup>12,13</sup> miR-204-5p is located on chromosome 9q21.11 within an intron of *TRPM3*, a gene that is downregulated in bladder cancer.<sup>14</sup> However, the biological functions of miR-204-5p and the genes it regulates are still unclear.

To gain insight into the biological roles of miR-204-5p, we analyzed the predicted targets of miR-204-5p and identified a well-known antiapoptotic gene—*BCL2*. In this study, we evaluated the direct interaction between miR-204-5p and *BCL2*, detected *BCL2* suppression, and measured the induced apoptosis in PCa cells with elevated miR-204-5p expression.

## 2. Methods

### 2.1. Construction of miRNA expression plasmids

Paired oligonucleotides consisting of mature miR-204-5p sequences were annealed and cloned into a small-RNA expression vector, pSM, as described previously.<sup>15</sup> This cloning step generated pSM-204 that expresses matured miR-204-5p. We also constructed two other miRNA expression vectors that expressed miR-15a and miR-214 as positive and negative controls,<sup>7</sup> namely, pSM-15 and pSM-214, respectively. The oligonucleotides used in this study are listed in Table 1.

### 2.2. Cell culture

Human PCa cell lines including PC3 (CRL-1435), CWR22Rv1 (Rv1, CRL-2505), and LNCaP (CRL-1740) were obtained from American Type Culture Collection (ATCC, Rockville, MD, USA), cultured in Roswell Park Memorial Institute (RPMI)-1640 medium, and maintained at 37°C under 5% CO<sub>2</sub>. Human 293T embryonic kidney cells (CRL-11268) were cultured in Dulbecco's modified Eagle's medium. Culture media were supplemented with 10% fetal bovine serum, 2mM GlutaMAX-I (Invitrogen, Carlsbad, CA, USA), 100 U/mL penicillin, and 100 µg/mL streptomycin. Normal prostate epithelial cells (PrEC) were cultivated in PrEGM BulletKit (Lonza, Basel, Switzerland) and maintained in accordance with the manufacturer's instructions.

### 2.3. Prediction of miR-204-5p target genes

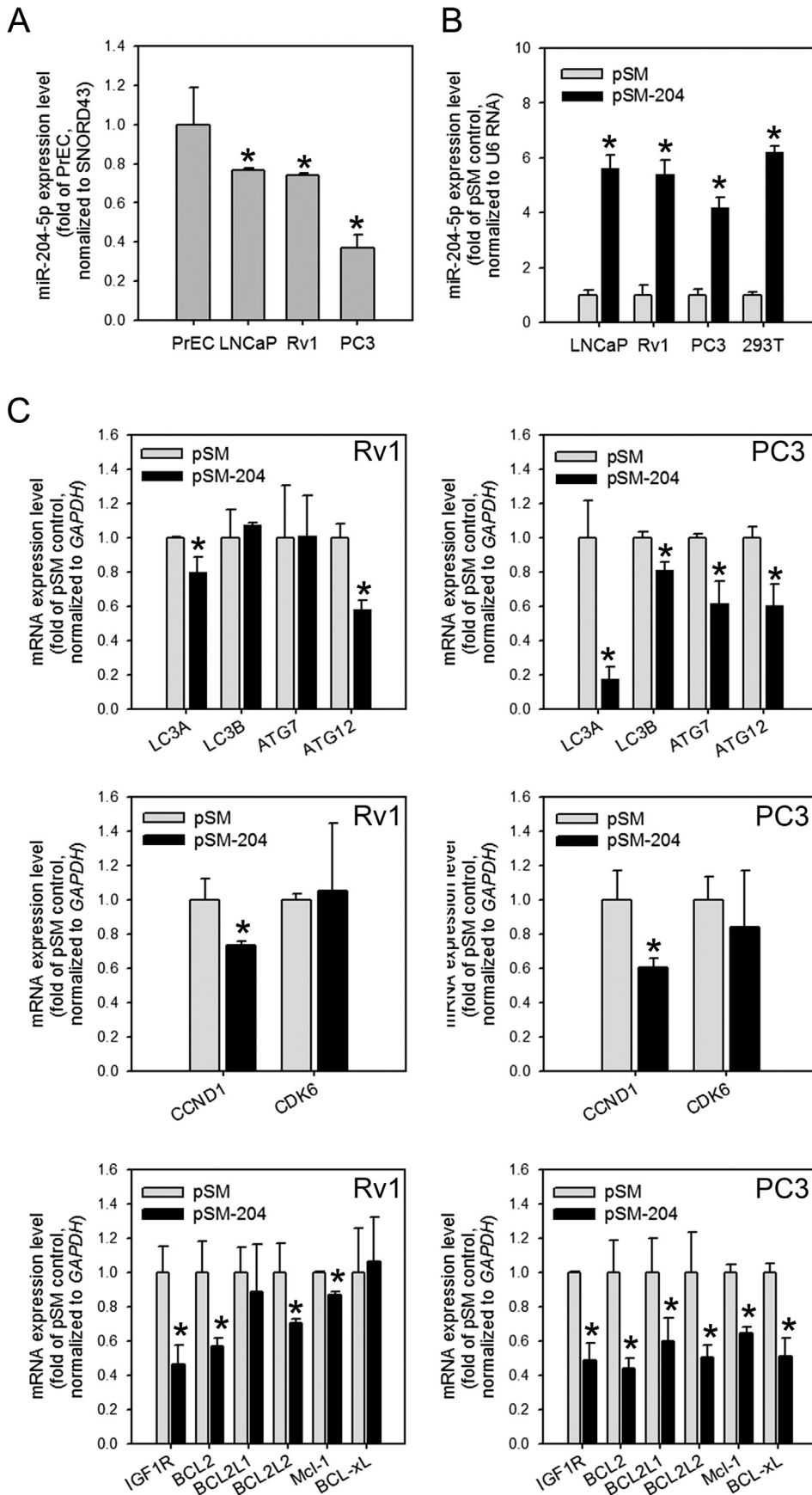
Potential miR-204-5p targets were predicted by computer-based programs as described in a previous study.<sup>15</sup> The autophagy-related genes (*LC3A*, *LC3B*, *ATG7*, and *ATG12*), cell-cycle-related genes (*CCND1* and *CDK6*), and antiapoptotic genes (*IGF1R*, *BCL2*, *BCL2L1*, *BCL2L2m Mcl-1*, and *BCL-xL*) are listed as predicted targeting genes for has-miR-204-5p in the TargetScan database. The secondary structure and the binding energy between miR-204-5p and *BCL2* or between miR-204-5p and the *BCL2L2* 3'-untranslated region (UTR) duplex were generated by RNAhybrid software (<http://bibiserv.techfak.uni-bielefeld.de/rnahybrid/>).<sup>16</sup> *BCL2* mRNA sequences of human (NM\_000633), chimpanzee (XM\_001145537), dog (NM\_001002949), cat (NM\_001009340), rat (NM\_016993), and mouse (NM\_009741) were retrieved from GenBank, and the alignment of these sequences was performed using Clustal Omega (<http://www.ebi.ac.uk/Tools/msa/clustalo/>).

**Table 1** List of oligonucleotides and polymerase chain reaction primer pairs used in this study.

Name	Sequences (5' → 3')
Oligonucleotides for construction of miRNA expression vectors	
Has-miR-204 (Top)	TGCTGTTCCCTTTGTCATCCTATGCTGTGTTTGGCCACTGACTGACAGGCATAGTGACAAAGGGAA
Has-miR-204 (Bot)	CCTGTTCCCTTTGTCATCCTATGCTGTGCTAGTCACTGAGTGGCCAAAACAGGCATAGGATGACAAAGGGAAAC
Has-miR-15 (Top)	TGCTGTAGCAGCACATAATGGTTTGTGGTTTGGCCACTGACTGACCACAAACCTATGTGCTGCTA
Has-miR-15 (Bot)	CCTGTAGCAGCACATAGGTTTGTGGTCACTGAGTGGCCAAAACACAAACCATTATGTGCTGCTAC
Has-miR-214 (Top)	TGCTGACAGCAGGCACAGACAGGCAGTGTGTTTGGCCACTGACTGACTGCCTGTGTGCCTGCTGT
Has-miR-214 (Bot)	CCTGACAGCAGGCACACAGGCAGTGTGCTGAGTGGCCAAAACACTGCCTGTCTGTGCCTGCTGTC
Stem-loop RT primers	
miR-204	GTT GGC TCT GGT GCA GGG TCC GAG GTA TTC GCA CCA GAG CCA ACA GGC AT
SNORD43	GTT GGC TCT GGT GCA GGG TCC GAG GTA TTC GCA CCA GAG CCA ACA ATC AG
Oligonucleotides for miRNA QPCR	
miR-204_F	GGG TTC CCT TTG TCA TCC T
SNORD43_F	GTG AAC TTA TTG ACG GGC G
Universal reverse primer	GTG CAG GGT CCG AGG T
<u>Probe</u> for miRNA QPCR	
UPL#21	/56-FAM/T+G+G +C+T+C +TG/3IABkFQ/
Oligonucleotides for reporter vector construction	
pmiR-204PTS (Top)	CTAGCAGGCATAGGATGACAAAGGGAAGATATCAGGCATAGGATGACAAAGGGAAAC
pmiR-204PTS (Bot)	TCGAGTTCCTTTGTCATCCTATGCTGTATCTTCCCTTTGTCATCCTATGCCTG
pmiR-204MTS (Top)	CTAGCTTCCCTTTGTCATCCTATGCTGTATCTTCCCTTTGTCATCCTATGCCTC
pmiR-204MTS (Bot)	TCGAGAGGCATAGGATGACAAAGGGAAGATATCAGGCATAGGATGACAAAGGGAAAG
pmiR-Bcl2-204TS (Top)	TCGAGGCAAAACGTCGAATCAGCTATTTACTGCCAAAGGGAAATATCATTATATGC
pmiR-Bcl2-204TS (Bot)	GGCCGCATAAATGATATTTCCCTTTGGCAGTAAATAGCTGATTCGACGTTTTTGGC
pmiR-Bcl2-204MTS (Top)	TCGAGGCAAAACGTCGAATCAGCTATTTACTGCC <span style="border: 1px solid black; padding: 0 2px;">TTTCCCTT</span> ATATCATTATATGC
pmiR-Bcl2-204MTS (Bot)	GGCCGCATAAATGATATAAGGGAAAGGCAGTAAATAGCTGATTCGACGTTTTTGGC
pmiR-15PTS (Top)	CTAGCCACAAACCATTATGTGCTGCTAGATATCCACAAACCATTATGTGCTGCTAC
pmiR-15PTS (Bot)	TCGAGTAGCAGCACATAATGGTTTGTGGATATCTAGCAGCACATAATGGTTTGTGG
pmiR-15MTS (Top)	CTAGCTAGCAGCACATAATGGTTTGTGGATATCTAGCAGCACATAATGGTTTGTGC
pmiR-15MTS (Bot)	TCGAGCACAAACCATTATGTGCTGCTAGATATCCACAAACCATTATGTGCTGCTAG
pmiR-Bcl2-15TS (Top)	TCGAGAAGTGATGAATATGGAATATCCAATCCTG <span style="border: 1px solid black; padding: 0 2px;">TGCTGCTA</span> TCCTGCCAAAAGC
pmiR-Bcl2-15TS (Bot)	GGCCGCTTTTGGCAGGATAGCAGCACAGGATTGGATATTCATATTCATCACTTC
pmiR-Bcl2-15MTS (Top)	TCGAGAAGTGATGAATATGGAATATCCAATCCTG <span style="border: 1px solid black; padding: 0 2px;">TAGCAGCA</span> TCCTGCCAAAAGC
pmiR-Bcl2-15MTS (Bot)	GGCCGCTTTTGGCAGGATGCTGTACAGGATTGGATATTCATATTCATCACTTC
QPCR primers	
HsBcl2-5QP1	CTGTGGTCCACCTGACCCTCCGC
HsBcl2-3QP1	CGTACAGTTCACAAAGGCATCCCAGC
HsBcl2l2-5QP1	GAGCCATATAGTTTCTTGGGA
HsBcl2l2-3QP1	TAGAATAAGTGGGGAGTGGGA
HsMcl1-5QP1	CCACCGGCGCCAAGGACACAAAG
HsMcl1-3QP1	AGCATGCCTTGAAGGCCGCTCTCG
HsCCND1-5QP1	CGTTGTACCTGTAGGACTCT
HsCCND1-3QP1	TGGCTTCATTGAGATTTGGAG
Hs-CDK6-5QP1	AGCAAGAACCCTTCTACCTATT
Hs-CDK6-3QP1	TGAAGACAGTAGCCTTAGAGATAA
Hs-ATG7-5QP1	GCTTGTCTTCCAAAGTTCTTG
Hs-ATG7-3QP1	ATGGTCTCATCATCGCTCAT
Hs-ATG12-5QP1	CATTCTTTGAAGATGCCTTGTGTT
Hs-ATG12-3QP1	AGTGGTAGTTTGTCTCTAAGTGTTT
Hs-LC3A-5QP1	CAGGTGCAAGGAGAAAGGAT
Hs-LC3A-3QP1	TGAGACAGTGTGAGAACTACC
Hs-BECN1-5QP1	CCAGAGCTACAACATGCCATC
Hs-BECN1-3QP1	TCAGAGAAGAAAGGGAAAGGAGTC
HsBad-5QP1	CATCATGGAGGCGCTGGGGC
HsBad-3QP1	TGCCGCATCTGCGTTGCTGTGCC
EGFP-5QP1	CGACGGCAACTACAAGAC
EGFP-3QP1	TAGTTGTACTCCAGCTTGTGC

miRNA targeting sites are underlined and miRNA seed sequences are boxed.

Bot = bottom; EGFP = enhanced green fluorescent protein; miRNA = microRNA; MTS = mutated target site; PTS = positive target site; QPCR = quantitative polymerase chain reaction; RT = reverse transcription.



## 2.4. Detection of miR-204-5p expression

We used a highly sensitive reverse transcriptase–polymerase chain reaction (RT-PCR) method to determine the expression level of miR-204-5p in PrEC, Rv1, and PC3 cells using Moloney murine leukemia virus RT (Epicentre) with stem–loop RT primer specific for miR-204-5p or *SNORD43* (internal control). Quantitative PCR (QPCR) to detect miR-204-5p or *SNORD43* was subsequently performed using miRNA-specific forward primers, miRNA universal reverse primer, and an UPL#21 probe. All oligonucleotides used in this study were synthesized by IDT (Integrated DNA Technologies, Singapore) and are listed in Table 1.

## 2.5. Real-time quantitative RT-PCR

Cells that reached approximately 70–80% confluences were transfected in 10-cm dishes with pSM-204 using a polymerase-based transfection reagent (Transfec 293, GeneDireX, Taipei, Taiwan). The expression level of miR-204-5p in transfected cells was measured as described previously.<sup>17</sup> To detect the expression levels of *BCL2*, *BCL2L2* (*Bcl-w*), *MCL1*, *CCND1*, *CDK6*, *ATG7*, *ATG12*, *LC3A*, *BECN1*, and *BAD*, first-strand complementary DNA (cDNA) was synthesized from total RNA (2 µg) using a first strand cDNA synthesis kit (Thermo Scientific) and oligo(dT) primers. QPCR was performed in a 20-µL reaction mixture that contained 0.5 µL of cDNA and 1× KAPA SYBR FAST universal QPCR master mix (Kapa Biosystems, Boston, MA, USA). Enhanced green fluorescent protein (EGFP) coexpressed with miR-204-5p was used as an internal standard to eliminate possible differences in transfection efficiency. The data were collected from triplicate experiments that were repeated three times using different batches of RNA samples. The data are expressed as mean ± standard deviation. The specific primer pairs used are listed in Table 1.

## 2.6. BCL2 3'-UTR reporter plasmid construction and luciferase assays

Double-stranded oligonucleotides containing 19 bases upstream and 11 bases downstream of miR-204-5p or miR-15a seed sequences of *BCL2* 3'-UTRs were synthesized, annealed, cloned downstream of the luciferase gene (*NheI*/*XhoI* sites) in the pmirGLO vector (Promega, Madison, WI, USA), and designated as "pmiR-Bcl2-204TS" and "pmiR-Bcl2-15TS," respectively. A similar cloning step using reverse seed sequences of miR-204-5p and miR-15a on the *BCL2* 3'-UTR yielded "pmiR-Bcl2-204MTS" and "pmiR-Bcl2-15MTS," respectively, which served as negative controls.

Positive and negative reporters were constructed using antisense and sense sequences of miR-204-5p and miR-15a, respectively, to generate positive target sites (PTs) and mutated target sites (MTs) on the reporter vectors. The 293T cells were cotransfected with miR-204-5p (pSM-204), miR-15a (pSM-15), or control (pSM) and reporter plasmids. Firefly and *Renilla* luciferase activities were measured consecutively at 24 hours post-transfection using a Promega Dual-luciferase kit according to the manufacturer's instructions. Relative protein levels were expressed as firefly/*Renilla* luciferase ratios.

## 2.7. Western blot analyses

Protein samples were collected at 96 hours post-transfection using radioimmunoprecipitation assay buffer containing 1× protease inhibitor cocktail. Protein concentrations were determined using a micro bicinchoninic acid protein assay kit, and the subsequent Western blot analyses were performed as described previously.<sup>15</sup> Band signals were acquired in the linear range of the scanner using densitometric software (TotalLab, Nonlinear Dynamics, NC, USA). The ratio of *BCL2* to EGFP band intensities was used to quantitate *BCL2* modulation by miR-204-5p.

## 2.8. Cell viability and apoptosis detection

Cell viability was measured with WST-1 reagent. To detect apoptosis, we evaluated cytochrome C release to the cytosol and caspase 3/7 activity in transfected cells. The protein fractions from cytosol were isolated using a mitochondria isolation kit (Thermo Scientific, MA, USA) and then analyzed by Western blot using anticypochrome C antibody and enhanced chemiluminescence as described earlier. Caspase 3/7 activity was assayed using an EnzChek Caspase-3 assay kit Number 2 (Invitrogen). Measured fluorescence levels were normalized to the fluorescence levels of nontransfected cell lysates, and caspase 3/7 activities were normalized to cell viability.

## 2.9. Statistical analysis

Data are presented as the means ± standard deviation of three independent experiments, each performed in triplicate. Student *t* test was used to differentiate the statistical significance. A value of  $p < 0.05$  was considered statistically significant.

**Figure 1** Downregulation of miR-204-5p in human prostate cancer cells, and enforced expression of miR-204-5p decreased the expression of antiapoptotic genes. (A) miR-204-5p was downregulated in prostate cancer cells compared with PrEC normal cells. (B) Enhanced expression of miR-204-5p in prostate cancer cells by transfection of pSM-204. (C) Decreased expression level of multiple-predicted miR-204-5p targeted genes in pSM-204-transfected Rv1 (left row) and PC3 (right row) cells. The data represent three independent experiments and are expressed as the mean percentage ± standard deviation relative to the vector-only control (pSM). \*  $p < 0.05$ . GAPDH = glyceraldehyde 3-phosphate dehydrogenase; mRNA = messenger RNA.

### 3. Results

#### 3.1. miR-204-5p was downregulated in PCa cells

To access the basal expression profile of miR-204-5p, we compared the endogenous level of miR-204-5p in PrEC, LNCaP, Rv1, and PC3 cells using a highly sensitive RT-QPCR method.<sup>18</sup> As shown in Figure 1A, the expression level of miR-204-5p was downregulated in LNCaP, Rv1, and PC3 cells compared with normal PrEC cells.

#### 3.2. Elevated level of miR-204-5p in pSM-204-transfected cells

To study the effect of miR-204-5p on the expression of putative targets in cancer cells, we increased the functional level of miR-204-5p in PCa cells (PC3, Rv1, and LNCaP). The embryonic kidney cells (293T) were included as reference cancer cells. As expected, the expression level of miR-204-5p was elevated in pSM-204-transfected cells when compared with control. As shown in Figure 1B, miR-204-5p transcripts were elevated to  $5.62 \pm 0.50$  folds,  $5.41 \pm 0.51$  folds,  $4.22 \pm 0.35$  folds, and  $6.21 \pm 0.24$  folds in LNCaP, Rv1, PC3, and 293T cells, respectively.

#### 3.3. Forced expression of miR-204-5p-downregulated genes involved in autophagy, cell cycle, and antiapoptosis

To investigate whether the expression of these predicted targeting genes was altered by enforced expression of miR-204-5p, the total RNA was isolated from Rv1 and PC3 cells transfected with pSM or pSM-204. The expression level of these mRNAs was then evaluated by subsequent QPCR. Our results demonstrated that multiple genes were downregulated by enforced expression of miR-204-5p in both Rv1 and PC3 cells, including *LC3A*, *ATG12*, *CCND1*, *IGF1R*, *BCL2*, *BCL2L2*, and *Mcl-1* (Figure 1C). Nevertheless, several genes such as *LC3B*, *ATG7*, *BCL2L1*, and *Bcl-xL* were only downregulated in PC3 cells.

#### 3.4. BCL2 was predicted as a target for miR-204-5p

An *in silico* strategy was used to identify putative miR-204-5p targets that may contribute to tumorigenesis. The prediction results and score from TargetScan are listed in Figure 2A. The *BCL2*-like 2 (*BCL2L2*) gene has been demonstrated to be an miR-204-5p target gene.<sup>19</sup> Therefore, we included the predicted results of miR-204-5p/*BCL2L2* as a reference. Conserved binding sites on the 3'-

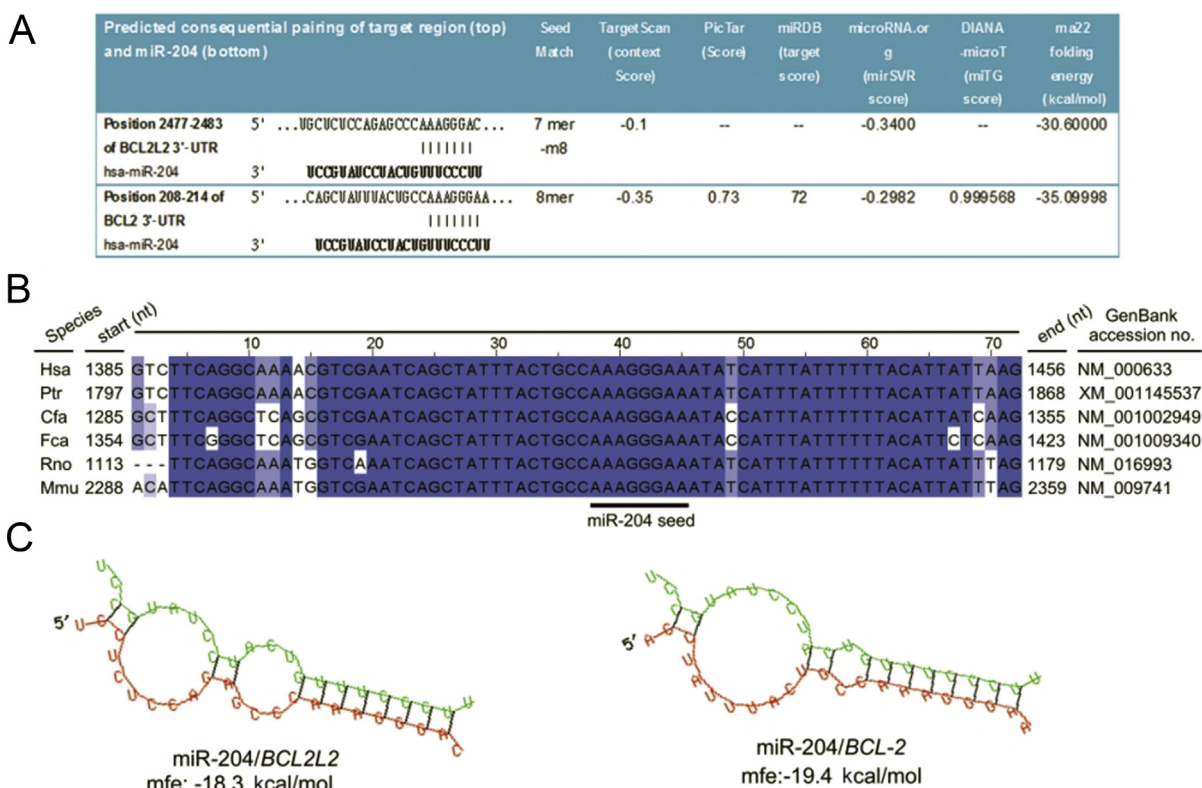


**Figure 2** BCL2 is a predicted target of miR-204-5p. (A) Putative binding sites of miR-204-5p in the *BCL2* and *BCL2L2* 3'-UTR regions as detected by several prediction databases. Those not listed in the databases are indicated by a dash. (B) *BCL2* 3'-UTR sequences that contain the putative miR-204-5p target site are highly conserved among vertebrate species. The miR-204-5p seed sequence is underlined. The listed partial *BCL2* 3'-UTR sequences are from the following species: human (Hsa); chimpanzee (Ptr); dog (Cfa); cat (Fca); rat (Rno); and mouse (Mmu). (C) Predicted RNA duplex structure of miR-204-5p/*BCL2* and miR-204-5p/*BCL2L2* binding generated by RNAhybrid. UTR = untranslated region.

UTR of *BCL2* across vertebrate species, including human, chimpanzee, dog, cat, rat, and mouse (Figure 2B), were retrieved from the TargetScan program. This observation suggests that miR-204-5p targeting of *BCL2* is preserved during evolution. The free energies of miR-204-5p binding to the *BCL2* and *BCL2L2* binding sites were calculated as  $-19.4$  kcal/mol and  $-18.3$  kcal/mol, respectively, using RNAhybrid software. The calculated binding energy further emphasized that the targeting sequence within the *BCL2* 3'-UTR likely binds to miR-204-5p. The predicted structures of miR-204-5p binding to *BCL2* and *BCL2L2* are shown in Figure 2C.

### 3.5. miR-204-5p interacts directly with the 3'-UTR of *BCL2*

To substantiate that miR-204-5p directly regulates *BCL2* through binding to its 3'-UTR targeting sequences, we tested whether the pSM-derived vectors could generate functionally mature miRNAs using luciferase reporter

assays. As illustrated in Figure 3A, luciferase reporter constructs bearing the PTS or mutative targeting site were constructed and designated as "pmiR-204-5pPTS" and "pmiR-204-5pMTS," respectively. In addition, to test whether miR-204-5p interacts directly with the putative targeting sequence on the 3'-UTR of *BCL2*, "pmiR-Bcl2-204TS" (bearing sequence from the 3'-UTR of *BCL2*) and "pmiR-Bcl2-204MTS" (bearing the same 3'-UTR sequence as pmiR-Bcl2-204TS except that the predicted miR-204-5p targeting seed sequence being mutated) were constructed. miR-15a with demonstrated targeting of *BCL2* was used as a positive control.<sup>5</sup> As shown in Figure 3B, luciferase activities decreased significantly in cells cotransfected with pSM-204 and pmiR-204-5pPTS. None of the miRNA expression plasmids had a regulatory effect on the pmirGLO reporter vector with the MTSs (Figure 3B). When we replaced the reporter vectors with pmiR-Bcl2-204TS and pmiR-Bcl2-15TS bearing the *BCL2* target sequences of miR-204-5p and miR-15a, respectively, the luciferase activities decreased (Figure 3C). We cloned reporter vectors (pmiR-

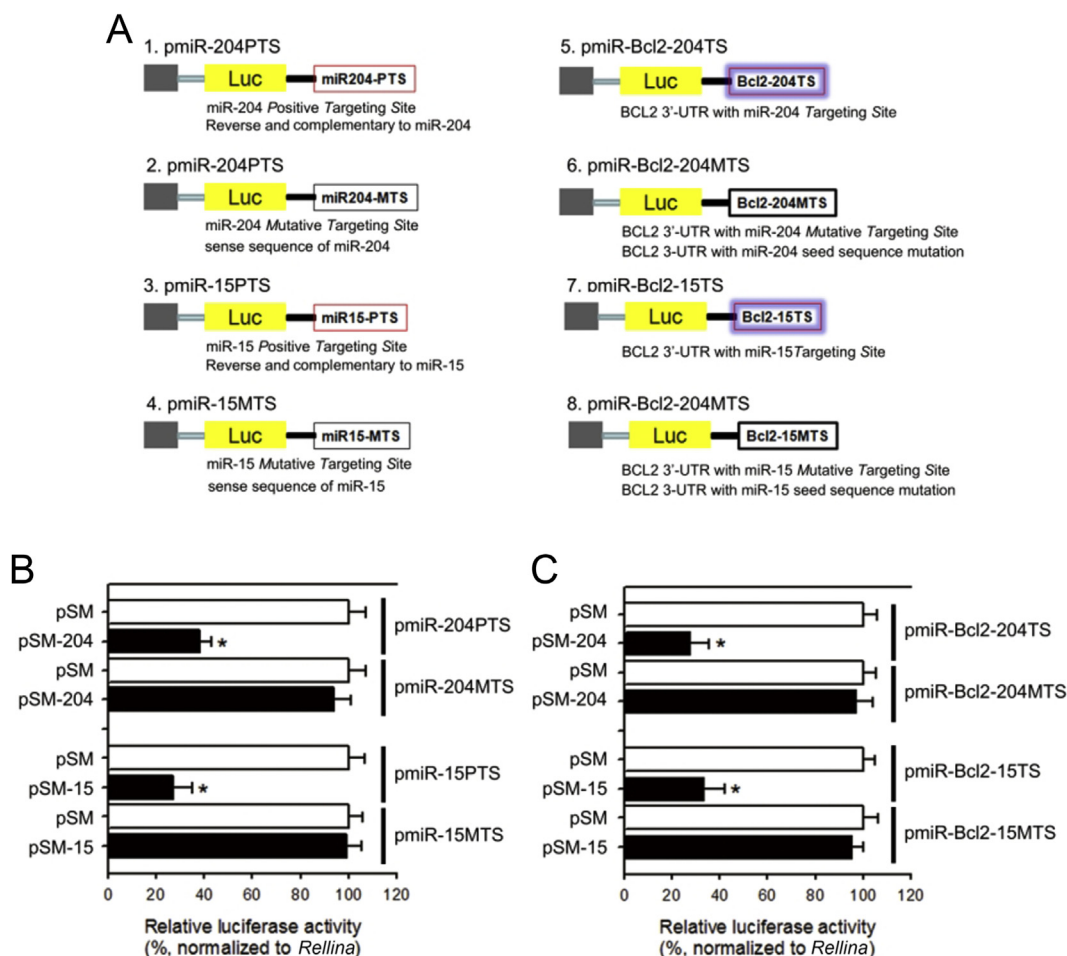


**Figure 3** Effect of the putative miR-204-5p targeting site derived from the *BCL2* 3'-UTR on luciferase expression. (A) An illustration of luciferase reporter constructs used in this study. Luciferase activity in 293T cells transiently cotransfected with pSM-204 expressing a sense strand of miR-204-5p and (B) the positive and negative control reporter vectors (PTS and MTS, respectively) or (C) the 3'-UTR of *BCL2* reporter vectors (TS and MTS). miR-15a with demonstrated targeting of *BCL2* was used as a positive control. The data are presented as the mean  $\pm$  standard deviation of three independent experiments, each performed in triplicate. \*  $p < 0.05$ . MTS = mutated target site; PTS = positive target site; UTR = untranslated region.

Bcl2-204MTS and pmiR-Bcl2-15MTS) that contained the reversed seed sequences of miR-204-5p and miR-15a on the 3'-UTR of *BCL2* as the MTSs. As expected, these mutants completely abolished the interaction between miR-204-5p and miR-15a with the 3'-UTR of *BCL2* (Figure 3C). These results indicated that pSM-204 and pSM-15 generate functional and mature miRNAs that directly interact with the 3'-UTR of *BCL2*.

### 3.6. Decreased BCL2 mRNA and protein levels in pSM-204-transfected cells

The *BCL2* mRNA expression level in pSM-204-transfected cells was measured by QPCR at 48 hours post-transfection. The *BCL2* mRNA expression levels were reduced by  $38.52 \pm 7.12\%$ ,  $42.00 \pm 8.12\%$ ,  $35.01 \pm 5.54\%$ , and  $35.12 \pm 6.18\%$  in LNCaP, Rv1, PC3, and 293T cells,

respectively, when compared with the vector-only control (Figure 4A). As a positive control, the mRNA expression levels of *BCL2L2* were reduced in all cell lines tested. We included miR-214, which has no detected target site in the 3'-UTR of *BCL2*, as a negative control. Therefore, *BCL2* expression was not altered by pSM-214 transfection (Figure 4A). To confirm that miR-204-5p modulates the *BCL2* system by specifically repressing *BCL2* expression, we analyzed the mRNA expression of *MCL-1*, another anti-apoptotic *BCL2* family member, and *BAD*, a proapoptotic protein that interacts with *BCL2*, in miR-204-5p-transfected cells. According to TargetScan, no predictive miR-204-5p target sites are present in the 3'-UTRs of *MCL-1* and *BAD*. Surprisingly, the *MCL-1* expression levels decreased in LNCaP and Rv1 cells transfected with pSM-204 (Figure 4A). However, in PC3 and 293T cells, the *MCL-1* level was not altered by pSM-204 transfection. In addition, decreased *BAD* levels were only detected in Rv1 cells transfected with

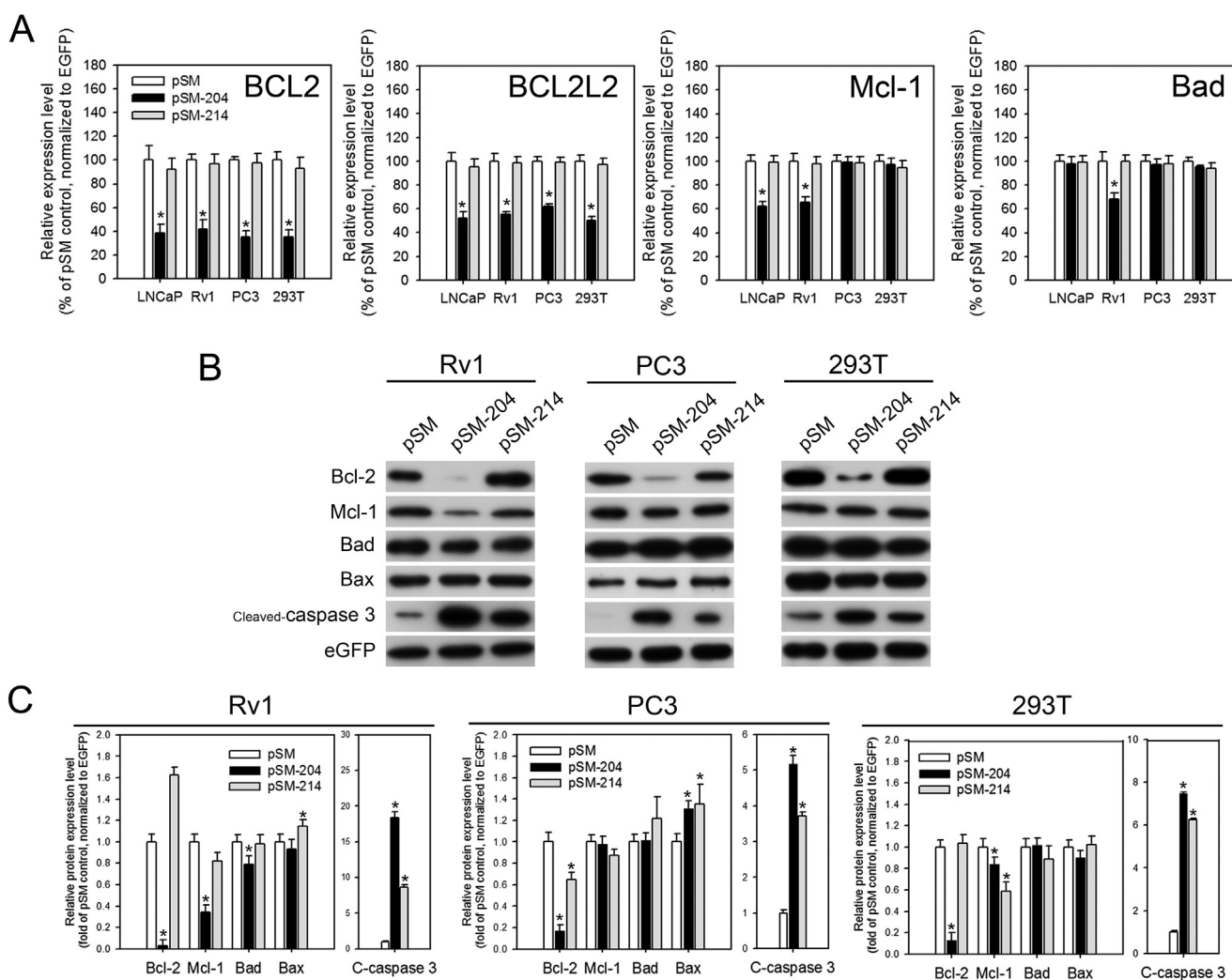


**Figure 4** BCL2 expression is repressed by miR-204-5p. (A) The relative messenger RNA (mRNA) levels of BCL2, Mcl-1, and Bad were measured in cells transfected with pSM-204 and pSM-214 and compared with vector-only controls (pSM) by quantitative polymerase chain reaction at 48 hours post-transfection. As a validated miR-204-5p target, the mRNA level of BCL2L2 was measured as a positive control. (B) Representative Western blot results of BCL2, MCL-1, BAD, BAX, and cleaved caspase 3 protein levels in pSM-204- and pSM-214-transfected cells. (C) The relative protein levels in each treatment from three independent experiments were quantified. \*  $p < 0.05$ . C-caspase = cleaved caspase; EGFP = enhanced green fluorescent protein.



pSM-204 (Figure 4A). Therefore, the decreased levels of *MCL-1* in LNCaP and Rv1 cells and *BAD* in Rv1 cells may be cell-specific secondary effects after pSM-204 transfection. Next, we examined the BCL2 protein level in response to elevated miR-204-5p expression. As shown in Figure 4B, the level of BCL2 decreased in pSM-204-transfected cells compared with the vector-only control (Rv1,  $32.26 \pm 10.21\%$ ; PC3,  $35.72 \pm 10.17\%$ ; and 293T,  $28.35 \pm 9.52\%$ ). These data suggest that miR-204-5p suppresses BCL2 expression at both RNA and protein levels.

### 3.7. BCL2 repression by miR-204-5p reduces cell viability and induces apoptosis in PCa cells

As shown in Figure 5A, cell viabilities decreased in cells transfected with pSM-204 (Rv1,  $57.31 \pm 2.82\%$ ; 293T,  $53.12 \pm 2.34\%$ ; and PC3,  $59.13 \pm 7.18\%$ ) compared with the vector-only control. To confirm that miR-204-5p is responsible for the decreased cell viability observed with BCL2 targeting, a rescue experiment was performed in which pSM-204 was cotransfected with reporter constructs that harbor the positive miR-204-5p target sequences (pmiR-204-5pPTS) or the 3'-UTR of *BCL2* (pmiR-Bcl2-204TS). These two reporters generated miR-204-5p target sequences to compete with exogenous miR-204-5p or endogenous *BCL2* transcripts. As shown in Figure 5A, the cotransfection of pSM-204 with pmiR-204-5pPTS restored cell viability in Rv1, PC3, and 293T cells, whereas the cotransfection of pSM-204 with pmiR-Bcl2-204TS partially rescued cell viability in these cells. These results indicate that miR-204-5p targets *BCL2* and leads to decreased cell viability; however, other miR-204-5p mRNA targets may also contribute to lost viability because the cell viability did not fully recover in cells cotransfected with pmiR-Bcl2-204TS and pSM-204. Furthermore, cell viability in cells treated with Z-VAD-FMK, a pan-caspase inhibitor, prior to the pSM-204 transfection was not reduced, suggesting that miR-204-5p-caused cell death is mainly through the activation of the caspase pathway. In Figure 5B, cytochrome C was released to the cytosol in pSM-204-transfected Rv1 and PC3 cells, indicating that miR-204 targeting of *BCL2* causes an imbalance of the antiapoptotic and proapoptotic protein levels and induces the mitochondria-dependent apoptotic pathway. Caspase 3/7 activation was detected in cells transfected with pSM-204 and could be suppressed by cotransfection with reporter constructs (Figure 5C).

## 4. Discussion

The imbalance of antiapoptotic and proapoptotic proteins plays an important role in cancer development and progression. BCL2 upregulation has been demonstrated in many cancer types.<sup>18</sup> BCL2 inhibits apoptosis by interacting with proapoptotic members of the BCL2 family, such as BAD, BAX, and BID. A decreased level of BCL2 disrupts the balance of antiapoptotic and proapoptotic homodimers, and thus, activates the apoptotic cascade.<sup>17</sup> BCL2 is highly expressed in androgen-independent PCa.<sup>20</sup> Therefore, BCL2 has become an attractive therapeutic target of cancer treatments.<sup>21</sup>

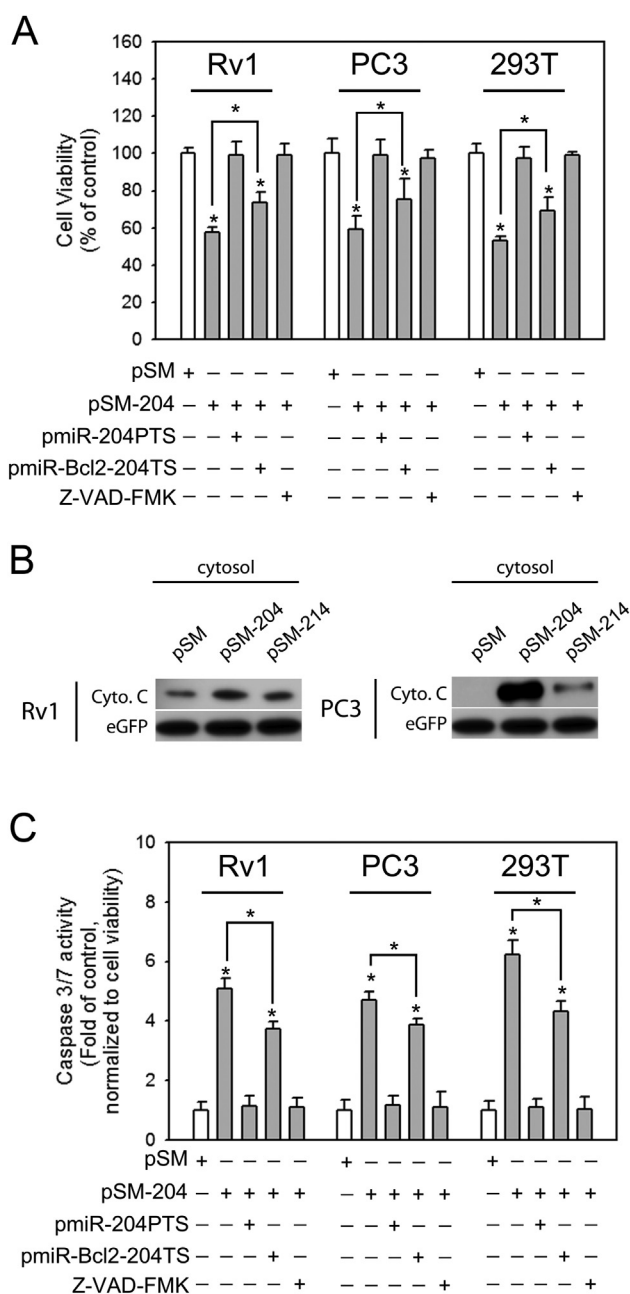


**Figure 5** Repression of BCL2 by miR-204-5p reduces cell viability and induces apoptosis. Cells were transfected with the indicated vectors. At 72 hours post-transfection, (A) cell viability, (B) cytosolic cytochrome C, and (C) caspase 3/7 activity were detected. Reporter vectors expressing a positive miR-204-5p target sequence (pmiR-204-5pPTS) or containing the BCL2 3'-UTR (pmiR-Bcl2-204TS) were cotransfected with pSM-204 in the rescue experiments. Cells were pretreated with  $10\mu\text{M}$  Z-VAD-FMK prior to the transfection. Enhanced green fluorescent protein served as loading controls for cytosolic proteins. \*  $p < 0.05$ . UTR = untranslated region.

miR-204-5p has been demonstrated to be involved in the regulation of multiple functions in different cell types of human. It was reported to target *TGF- $\beta$*  receptor 2 and *SNAIL2* in retinal pigmented epithelium, which led to a

decrease in transepithelial resistance.<sup>22</sup> miR-204-5p has also been found to be highly abundant in distal axons, suggesting its potential role in neuronal growth and development.<sup>23</sup>

Downregulation of miR-204-5p has been reported in human breast cancer,<sup>24</sup> bladder cancer,<sup>13,25</sup> renal clear cell carcinoma,<sup>26</sup> head and neck tumor,<sup>27</sup> leukemia,<sup>28</sup> and endometrioid adenocarcinoma.<sup>10</sup> Here, we showed that manipulation of miR-204-5p expression in PCa cells induces apoptosis by directly targeting BCL2. These results indicate that the interaction between miR-204-5p and BCL2 may be universal. As a positive control, we also demonstrated that another antiapoptotic protein, BCL2L2, was targeted by miR-204-5p. Interestingly, MCL-1 expression levels were altered in miR-204-5p-transfected LNCaP and Rv1 cells. Because there is no predictive target site of miR-204-5p on the 3'-UTR of *MCL-1*, the decreased level of *MCL-1* is likely to be a secondary effect of miR-204-5p expression.

The expression of the proapoptotic gene *BAD* was not affected by the elevated level of miR-204-5p in LNCaP, PC3, and 293T cells, while decreased levels of *BAD* were detected in Rv1 cells. This observation is not consistent with the common knowledge that *BAD* promotes apoptosis. The decreased level of *BAD* observed in Rv1 cells is likely to be a result of apoptosis induction by miR-204-5p because apoptosis induction was detected in all tested cell lines.

The elevation of miR-204-5p expression significantly reduced the cell viability of all transfected cancer cell lines. Cell viabilities were restored fully or partially by the cotransfection of reporter constructs bearing a positive miR-204-5p target site (pmiR-204-5pPTS) or a *BCL2* target site (pmiR-Bcl2-204TS), respectively. These results indicate that *BCL2* is not the only target of miR-204-5p responsible for the lost cell viability. Indeed, as mentioned earlier, *BCL2L2* was reported to be an antiapoptotic target of miR-204-5p in human trabecular meshwork (HTM) cells. The elevation of miR-204-5p in HTM cell lines also induced apoptosis and caused cell death.<sup>19</sup> This finding further supports the idea that miR-204-5p functions as a tumor-suppressing miRNA by targeting antiapoptotic genes.

The limitation of the study is that it was a cell-based study. Hence, future studies using clinical samples directed toward the elucidation of the relationship between miR-204-5p and antiapoptotic genes may provide further insights into the design of novel molecular therapies for PCa and, more importantly, into the inhibition of cancer progression.

## 5. Conclusion

Our results showed that *BCL2* is a direct target of miR-204-5p in human PCa cells. miR-204-5p overexpression resulted in the decreased level of *BCL2*, which in turn increased apoptosis and decreased cellular viability. Taken together, miR-204-5p can be a possible novel molecular therapeutic candidate for PCa.

## Acknowledgments

We thank Dr Guangwei Du (University of Texas Health Science Center at Houston, TX, USA) for kindly providing the

pSM plasmids. The study was supported by grants NSC102-2314-B-341-003-MY3 (to J.F.L.) from the Ministry of Science and Technology, and SKH-8302-101-0202 (to J.F.L.) and SKH-8302-102-0201 (to T.I.S.) from Shin-Kong Wu Ho-Su Memorial Hospital, Taiwan.

## References

1. Pu YS. Prostate cancer in Taiwan: epidemiology and risk factors. *Int J Androl.* 2000;23:34–36.
2. Health Promotion Administration. *Cancer Registry Annual Report, Republic of China, 2000.* Taipei, Taiwan: Health Promotion Administration, Ministry of Health and Welfare, P.R. China; 2012.
3. Jerónimo C, Bastian PJ, Bjartell A, et al. Epigenetics in prostate cancer: biologic and clinical relevance. *Eur Urol.* 2011;60:753–766.
4. Ambs S, Prueitt RL, Yi M, et al. Genomic profiling of microRNA and messenger RNA reveals deregulated microRNA expression in prostate cancer. *Cancer Res.* 2008;68:6162–6170.
5. Porkka KP, Pfeiffer MJ, Waltering KK, Vessella RL, Tammela TL, Visakorpi T. MicroRNA expression profiling in prostate cancer. *Cancer Res.* 2007;67:6130–6135.
6. Bartel DP. MicroRNAs: genomics, biogenesis, mechanism, and function. *Cell.* 2004;116:281–297.
7. Cimmino A, Calin GA, Fabbri M, et al. miR-15 and miR-16 induce apoptosis by targeting BCL2. *Proc Natl Acad Sci U S A.* 2005;102:13944–13949.
8. Poy MN, Eliasson L, Krutzfeldt J, et al. A pancreatic islet-specific microRNA regulates insulin secretion. *Nature.* 2004;432:226–230.
9. Lee YS, Dutta A. MicroRNAs in cancer. *Annu Rev Pathol.* 2009;4:199–227.
10. Wu W, Lin Z, Zhuang Z, Liang X. Expression profile of mammalian microRNAs in endometrioid adenocarcinoma. *Eur J Cancer Prev.* 2009;18:50–55.
11. Garzon R, Garofalo M, Martelli MP, et al. Distinctive microRNA signature of acute myeloid leukemia bearing cytoplasmic mutated nucleophosmin. *Proc Natl Acad Sci U S A.* 2008;105:3945–3950.
12. Chen L, Yan HX, Yang W, et al. The role of microRNA expression pattern in human intrahepatic cholangiocarcinoma. *J Hepatol.* 2009;50:358–369.
13. Tsai T-F, Lin Y-C, Chen H-E, Chou K-Y, Lin J-F, Hwang TIS. Involvement of the insulin-like growth factor I receptor and its downstream antiapoptotic signaling pathway is revealed by dysregulated microRNAs in bladder carcinoma. *Urol Sci.* 2014;25:58–64.
14. Dyrskjot L, Kruhoffer M, Thykjaer T, et al. Gene expression in the urinary bladder: a common carcinoma *in situ* gene expression signature exists disregarding histopathological classification. *Cancer Res.* 2004;64:4040–4048.
15. Lin CJ, Gong HY, Tseng HC, Wang WL, Wu JL. miR-122 targets an anti-apoptotic gene, *Bcl-w*, in human hepatocellular carcinoma cell lines. *Biochem Biophys Res Commun.* 2008;375:315–320.
16. Rehmsmeier M, Steffen P, Hochmann M, Giegerich R. Fast and effective prediction of microRNA/target duplexes. *RNA.* 2004;10:1507–1517.
17. Humlová Z. Protooncogene *bcl-2* in process of apoptosis. Review article. *Sb Lek.* 2002;103:419–425.
18. Yip KW, Reed JC. Bcl-2 family proteins and cancer. *Oncogene.* 2008;27:6398–6406.
19. Li G, Luna C, Qiu J, Epstein DL, Gonzalez P. Role of miR-204 in the regulation of apoptosis, endoplasmic reticulum stress response, and inflammation in human trabecular meshwork cells. *Invest Ophthalmol Vis Sci.* 2011;52:2999–3007.

20. McDonnell TJ, Troncso P, Brisbay SM, et al. Expression of the protooncogene bcl-2 in the prostate and its association with emergence of androgen-independent prostate cancer. *Cancer Res.* 1992;52:6940–6944.
21. Adams JM, Cory S. Bcl-2-regulated apoptosis: mechanism and therapeutic potential. *Curr Opin Immunol.* 2007;19:488–496.
22. Wang FE, Zhang C, Maminishkis A, et al. MicroRNA-204/211 alters epithelial physiology. *FASEB J.* 2010;24:1552–1571.
23. Natera-Naranjo O, Aschrafi A, Gioio AE, Kaplan BB. Identification and quantitative analyses of microRNAs located in the distal axons of sympathetic neurons. *RNA.* 2010;16:1516–1529.
24. Baffa R, Fassan M, Volinia S, et al. MicroRNA expression profiling of human metastatic cancers identifies cancer gene targets. *J Pathol.* 2009;219:214–221.
25. Catto JW, Miah S, Owen HC, et al. Distinct microRNA alterations characterize high- and low-grade bladder cancer. *Cancer Res.* 2009;69:8472–8481.
26. Mikhaylova O, Stratton Y, Hall D, et al. VHL-regulated MiR-204 suppresses tumor growth through inhibition of LC3B-mediated autophagy in renal clear cell carcinoma. *Cancer Cell.* 2012; 21:532–546.
27. Lee Y, Yang X, Huang Y, et al. Network modeling identifies molecular functions targeted by miR-204 to suppress head and neck tumor metastasis. *PLoS Comput Biol.* 2010;6:e1000730.
28. Volinia S, Galasso M, Costinean S, et al. Reprogramming of miRNA networks in cancer and leukemia. *Genome Res.* 2010; 20:589–599.